Application of COMSOL Multiphysics in the Simulation of Magnesium Refining and Production

Xiaofei Guan[1], Eric Gratz[1], and Uday B. Pal[*1,2]

[1]Division of Materials Science and Engineering, Boston University, Brookline, MA 02446, USA
[2]Department of Mechanical Engineering, Boston University, Boston, MA 02215, USA
*Corresponding author: 750 Commonwealth Avenue, Boston, MA 02215, USA, upal@bu.edu

Abstract: Computational fluid dynamics (CFD) modeling is a useful tool to gain an insight into various high temperature metallurgical processes such as the magnesium refining and the magnesium solid oxide membrane (SOM) electrolysis. In both processes, argon gas was used to stir the molten salt (flux) in order to improve the transport of magnesium vapor out of the flux and achieve chemical homogeneity in the molten flux. In this study, the flow behavior of the flux and its effect on the mass transport of magnesium were simulated, and the flow behavior of the flux under reduced pressure stirred by argon was also investigated using COMSOL multiphysics. An optimized design of the magnesium production system was proposed based on the modeling results.

Keywords: Magnesium, refining, electrolysis, stirring, molten salts

1. Introduction

Magnesium (Mg) is the least dense engineering material, with an excellent stiffness-to-weight ratio. The wide spread use of magnesium as a structural and functional material is driving the development of new cost effective and environmentally friendly methods of primary magnesium production and recycling. Recently, magnesium has been refined from the magnesium-aluminum (Al) alloy by a novel refining process: dissolving magnesium and its oxide into a molten MgF_2-CaF_2 flux, followed by argon-assisted evaporation of dissolved magnesium and subsequent condensing of the magnesium vapor. Further details of the refining process are described elsewhere [1]. In addition to refining, the production of magnesium by direct electrolysis of its oxide using the SOM process has been shown to be effective on a laboratory scale [2], [3]. In the SOM process a yttria-stabilized zirconia (YSZ) tube is immersed in the MgO-MgF_2-CaF_2 flux. The anode is liquid silver contained in the YSZ tube, the cathode is the crucible wall which holds the flux. When an applied potential exceeds the magnesium oxide dissociation potential the magnesium cations travel to the cathode where they are reduced, and the oxygen anions travel through the YSZ to the anode where they are oxidized. The magnesium produced evolves as a gas and is transported to a lower temperature container where it is cooled and collected. In both refining and production processes, argon gas was used to stir the flux in order to improve the transport of magnesium vapor out of the flux. In the SOM electrolysis process, the stirring of the flux also improves the diffusion and convection of magnesium cations to the cathode.

COMSOL multiphysics provide useful insights for the research and development of various high temperature metallurgical processes. It has been proven to be a powerful tool for simulating the argon gas-stir induced flow in the metal bath of the basic oxygen steelmaking process [4].

In this paper, the flow behavior of the molten flux and its effect on the mass transport of magnesium were simulated, and the flow behavior of the molten flux under reduced pressure stirred by argon was investigated using COMSOL multiphysics as well.

2. Governing Equations

For the refining process, the laminar bubbly flow mode taken from COMSOL Multiphysics 4.2a CFD module, was utilized to model the flow induced by the argon gas stirring. The bubbly flow physics interface makes it easy to set up a multiphase flow model for the argon gas bubbles rising through the molten flux. The bubbly flow mode tracks the average phase concentration rather than each bubble in detail, and is therefore well suited to model the flow of the molten flux [5]. It solves for the properties relevant to the processes discussed in this work such as the liquid velocity, gas velocity, and the volume fraction of the gas phase. The bubbly flow mode

was then coupled with the transport of diluted species mode to simulate the mass transport of magnesium.

For the SOM electrolysis process, the laminar bubbly flow mode, taken from COMSOL Multiphysics 3.5a Chemical Engineering module, was utilized to model the flow behavior of the molten flux.

In this section the conservation equations of momentum and mass are described, respectively.

2.1 Conservation of Momentum

The momentum transport equation for the mixture of the molten flux and the argon gas is:

$$\phi_l \rho_l \frac{\partial \vec{u}_l}{\partial t} + \phi_l \rho_l \vec{u}_l \cdot \nabla \vec{u}_l = -\nabla p + \nabla \cdot \left[\phi_l \eta_l \left(\nabla \vec{u}_l + \nabla \vec{u}_l^{\,T} \right) \right] + \phi_l \rho_l \vec{g} \quad (1)$$

where ϕ_l denotes the volume fraction of the molten flux, ρ_l the molten flux's density (2600 kg/m^3 at 1150 ℃), $\vec{u}_l$ the molten flux velocity (m/s), p pressure (Pa), η_l the molten flux's dynamic viscosity (0.032 Pa s [6]) and $\vec{g}$ the gravity vector (9.8 m/s^2).

2.2 Conservation of Mass

The magnesium transport through the flux is modeled with the transport of diluted species shown in Equation 2.

$$\frac{\partial C_{Mg}}{\partial t} + \nabla \left(-D_{Mg} \nabla C_{Mg} \right) + \vec{u}_l \cdot \nabla C_{Mg} = R_{Mg} \quad (2)$$

where C_{Mg} is the magnesium molar concentration in the molten flux, D_{Mg} is the diffusion coefficient (assumed to be 5×10^{-9} m^2/s), R_{Mg} is the rate of magnesium phase transition from liquid to vapor. Magnesium dissolved in the molten flux becomes vapor when it meets argon, because the partial pressure of magnesium dissolved in flux is higher than that in argon. In addition, magnesium can vaporize when its concentration exceeds its solubility in flux. A suggested expression of R_{Mg} could be

$$R_{Mg} = -k C_{Mg} \phi_g \quad (3)$$

where k is a positive coefficient (assumed to be 1), C_{Mg} is the magnesium concentration, and ϕ_g is the volume fraction of argon. Equations (1) and (2) can be coupled together by the same terms $\vec{u}_l$ and ϕ_g.

3. Model Descriptions

3.1 Refining Process

For the refining process, Figure 1 depicts the geometry of the molten flux system for finite element analysis (FEA). The cylinder hole on the top surface represents the bubbling tube; the hollow space inside the flux represents the inverted crucible and the alloy crucible, between which there is a gap as labeled in Figure 1 (a).

The model consists of one domain with an inlet of argon (the bottom of the bubbling tube) and another inlet of magnesium (the gap between the inverted crucible and the alloy crucible). The molten flux has a diameter of 2.64 inches and a height of 3.5 inches. The model uses a predefined mesh of normal element size.

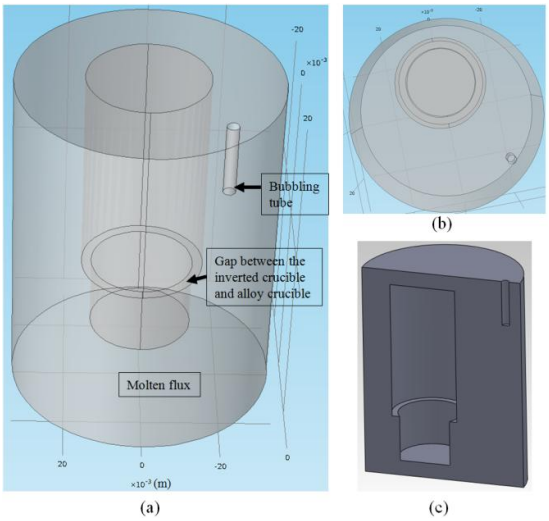

Figure 1. (a) The geometry of the molten flux system (b) A top view of the geometry of the molten flux system. (c) A full section view of the molten flux system.

The model assumes the following:

(1) Constant temperature (1150 ℃), and flux density and viscosity throughout the system.

(2) In the refining experiment, there were a reference rod and a venting tube. Here their

effect on the molten flux flow is ignored, and therefore they are not drawn in Figure 1.

(3) The wall thickness of the bubbling tube is neglected. The argon gas bubbler size is assumed to be half of the inner diameter (0.125 inch) of the bubbling tube, because there is a notch at the gas outlet of the bubbling tube in experiment.

3.1.1 Boundary Conditions

The following boundary conditions are adopted in the simulation. For the laminar bubbly flow mode,

(1) The bubbling tube bottom is the argon inlet with a flow rate of 20 cc/min, and there is no liquid slip.

(2) The top surface of the molten flux is the outlet of argon, and there is liquid slip.

(3) The pressure at the top surface of the molten flux is 1 atm.

(4) At the remaining walls, there is no gas flow or liquid slip.

For the transport of diluted species mode,

(1) The gap between the inverted crucible and the alloy crucible is the inlet of the magnesium with a concentration of 224.57 mol/m^3.

(2) At the top surface of the molten flux, the magnesium concentration is set to be zero.

(3) At the remaining walls, there is no magnesium flux.

3.1.2 Initial Conditions

The following initial conditions are adopted in the simulation. For the laminar bubbly flow mode, the initial molten flux velocity field is zero.

For the transport of diluted species, the velocity field used is from the results of the laminar bubbly flow mode. The initial magnesium concentration throughout the flux is zero.

3.1.3 Computing

The flow profile of the molten flux is solved in transient mode with a solution time of 20 seconds and a time step of 0.1 second. The solution of the molten flux flow at 20 seconds is used as the initial condition for simulating a time-dependent solution in case of the transport of magnesium.

3.2 SOM Electrolysis Process

Figure 2 depicts the geometry of the molten flux system for the SOM electrolysis process. The model consists of one domain with an argon gas inlet (the bottom of the bubbling tube). The molten flux has a diameter of 2.64 inches and a height of 1.8 inches. The model uses a predefined mesh of normal element size. Similar assumptions to the refining process are made.

(1) Constant temperature, and flux viscosity and density throughout the system.

(2) At reduced pressure, the bubble diameter was calculated according to ideal gas law.

$$\left.\begin{aligned} P_i V &= nRT \\ V &= \frac{\pi d^3}{6} \end{aligned}\right\} \Rightarrow d = \left(\frac{6nRT}{\pi P_i}\right)^{\frac{1}{3}} \qquad (4)$$

where d is the argon bubble diameter, n is the moles of argon in a bubble, and it is calculated to be 1.795×10^{-8} mole for a bubble with a diameter of 1.5875 mm at 1atm, R is the ideal gas constant (8.314 J/(mol K)), T is the temperature of the argon (1150 ℃), and P_i is the pressure inside the argon bubble. The bubble pressure depends on the pressure above the flux, the hydrostatic pressure and the pressure due to the surface tension of the flux. The model assumes the contribution to the bubble pressure from the hydrostatic pressure and surface tension is negligible.

Equation 4 shows that the bubble diameter d is a function of the pressure inside the argon bubble P_i. The bubble diameters at different bubble pressures are shown in Table 1.

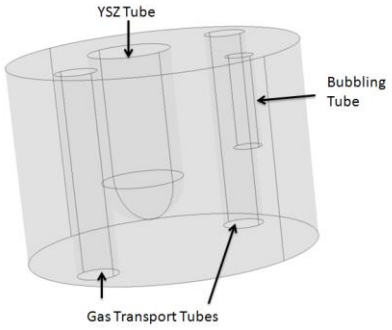

Figure 2. The simulating domain of the SOM electrolysis process.

Table 1: Bubble diameters at different pressures

Bubble pressure (atm)	Bubble diameter (mm)
1	1.5875
0.8	1.7100
0.6	1.8822
0.4	2.1546

3.2.1 Boundary Conditions

The following boundary conditions are adopted in the simulation.

(1) The bubbling tube bottom is the inlet of argon and there is no liquid slip.

(2) The top surface of the molten flux is the outlet of argon, and there is liquid slip.

(3) The pressure at the top surface of the molten flux is set to be different values as shown in Table 1.

(4) At the remaining walls, there is no gas flow or liquid slip.

3.2.2 Initial Conditions

For the laminar bubbly flow mode, the initial molten flux velocity field is zero.

3.2.3 Computing

The flow profile of the molten flux is solved in transient mode with a solution time of 10 seconds and a time step of 0.1 second.

4. Results and Discussions

4.1 Refining Process

Figure 3 and 4 show the flow profile of the molten flux with the argon flow rate of 20 cc/min after 20 seconds. The flow profile becomes quite stable after 10 seconds. Figure 3 shows the flow profile of the molten flux on the surface where the maximum velocity magnitude of the molten flux is 5.61 cm/s. The arrows on the top surface represent the magnitude and the direction of the velocity. Figure 4 shows the molten flux flow profile of the molten flow on the vertical slices where the maximum velocity magnitude of the molten flux is 5.91 cm/s. The argon bubbling induces a circulating motion of the flux on the upper part shown in Figure 4, which facilitates the convection of magnesium. There is a dead zone at the bottom part of the molten flux, which means the velocity magnitude is almost zero and the flux is stagnant. The transport of magnesium mainly depends on the diffusion at the very bottom zone.

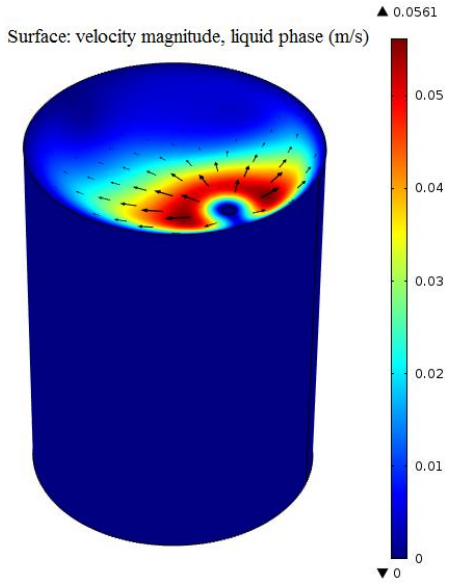

Figure 3. The molten flux flow profile on the surface.

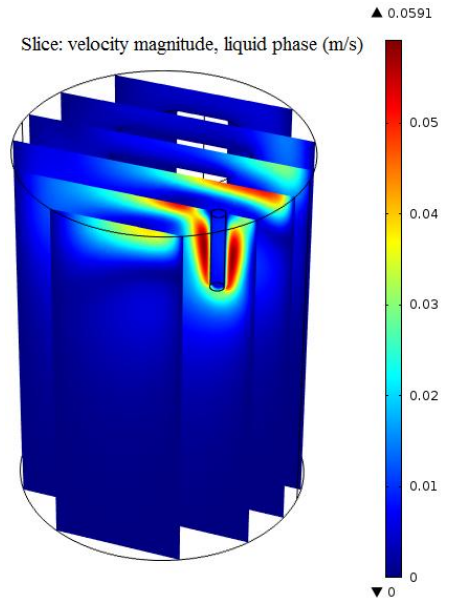

Figure 4. The molten flux flow profile on the slices.

Figure 5 shows the argon gas volume fraction on the vertical slices. The maximum gas volume fraction at the front slice is 17.46%. Figure 6 shows the magnesium concentration distribution in the flux on the middle vertical slice after 7 hours. The magnesium diffuses out

of the gap between the inverted crucible and the alloy crucible, and transports through the flux due to the diffusion and convection. As shown in Figure 6, the magnesium at the side close to the bubbling tube rises up, and the magnesium at the other side away from the bubbling tube goes downward; the magnesium transport follows the circulation motion of the molten flux.

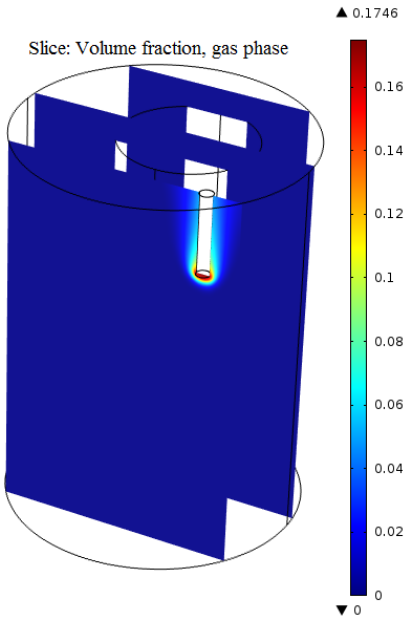

Figure 5. The argon gas volume fraction on the slices.

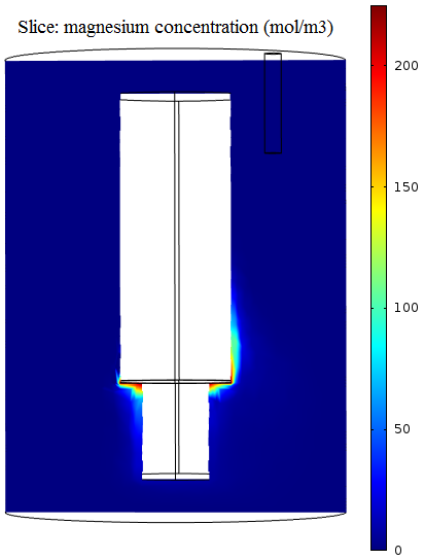

Figure 6. The magnesium distribution on the middle vertical slice.

In the refining experiment, magnesium dissolved in flux can vaporize when its concentration exceeds its solubility limit in the flux, which is not considered in this modeling.

4.2 SOM Electrolysis Process

When the flux is stirred with argon at 100 cc/min the maximum velocity of the flux is 18.54 cm/s near the bubbling tube, as shown in Figure 7. However, as the distance from the bubbling tube increased the velocity dropped to a less than 2 cm/s, suggesting that magnesium transport out of the flux is greatest near the bubbling tube.

It should be noted that the diameter of the bubbling tube here is 0.25 inch, and the bubble diameter is also set to be 0.25 inch. The depth of the bubbling tube in flux is 0.8 inch.

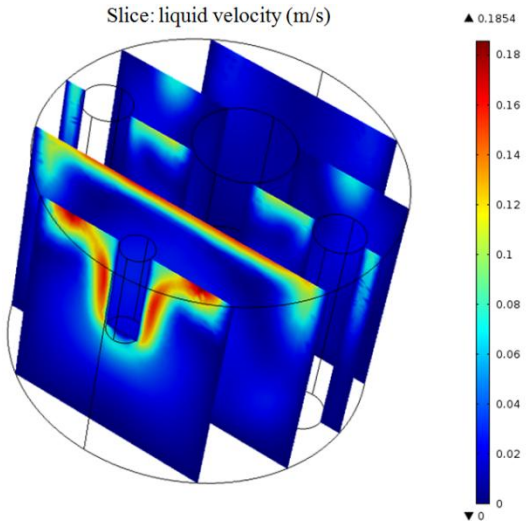

Figure 7. Flow behavior of the molten flux at 1 atm when stirred at 100 cc/min.

4.2.1 SOM Electrolysis Process at Reduced Pressure

Since magnesium has a slight solubility in the flux it is advantageous to run electrolysis at reduced pressure. Changing the pressure of the system affects the flow behavior of the flux.

In the low pressure case the effect of the YSZ tube and the venting tubes on the molten flux flow is ignored. The bubbling tube diameter is reduced to 0.125 inch. The bubble diameter is set to be half of the bubbling tube diameter due to the notch in the bubbling tube. The depth of the

bubbling tube in flux is 1.5 inches. The results from the model are comparative, to simulate the effect of reducing the system pressure. The effect of argon stirring on the flow behavior of the molten flux is modeled at four pressures, 1 atm, 0.8 atm, 0.6 atm and 0.4 atm.

The effect argon stirring has on the flux at 1 atm is shown in Figure 8; Figure 9-Figure 11 show the effect of argon stirring at reduced pressures. In all the four cases the argon flow rate is 15 cc/min.

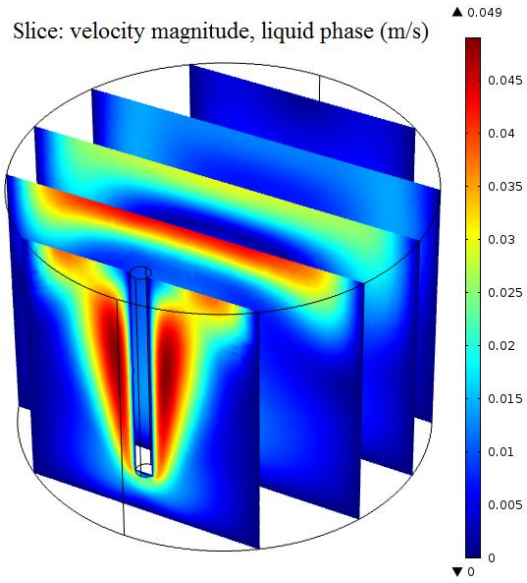

Figure 8. Flow behavior of the molten flux at 1 atm.

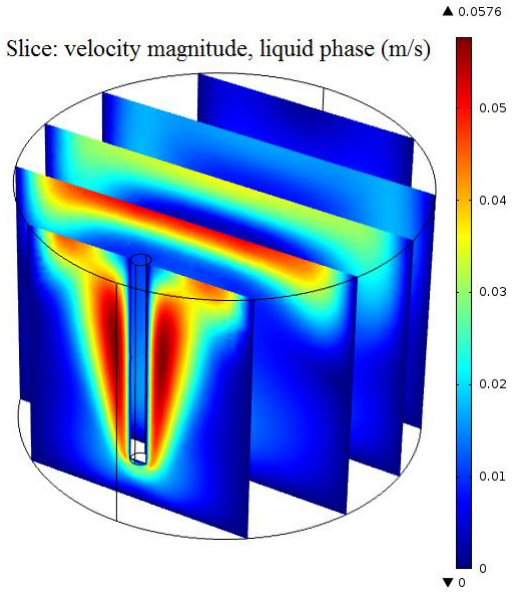

Figure 9. Flow behavior of the molten flux at 0.8 atm.

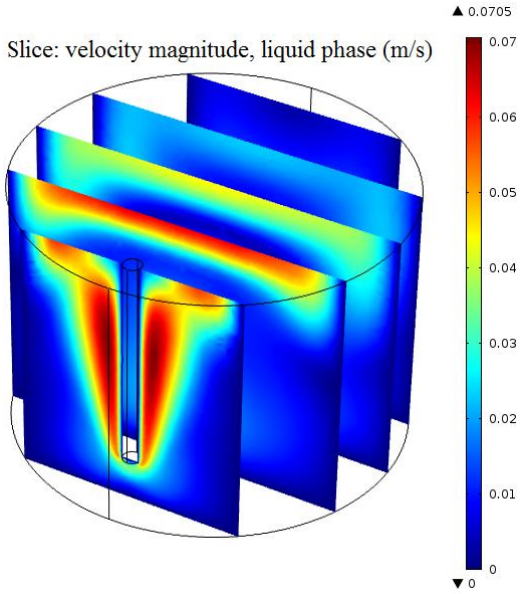

Figure 10. Flow behavior of the molten flux at 0.6 atm.

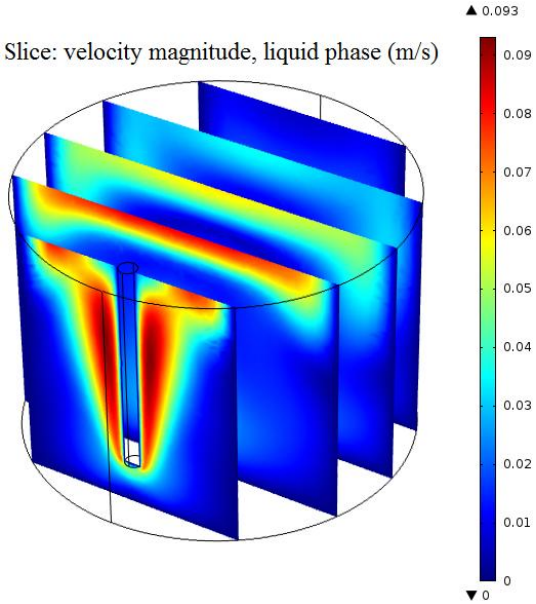

Figure 11. Flow behavior of the molten flux at 0.4 atm.

It is observed that as the pressure of the system drops and the argon bubble size increases the velocity of the flux also increases from a maximum velocity of 4.9cm/s at 1 atm to 9.3 cm/s at 0.4 atm. The relationship between the maximum velocity magnitude and the bubble pressure is drawn in Figure 12. This indicates that as the pressure in the system is lowered, the

rate of argon stirring can be decreased to achieve similar flow behavior. SOM electrolysis experiments were carried out at 0.1 atm, and the argon flow rate was 15 cc/min [7]. Future modeling work will investigate the effect of argon stirring at this pressure. However, in this case the bubbly flow mode cannot be used.

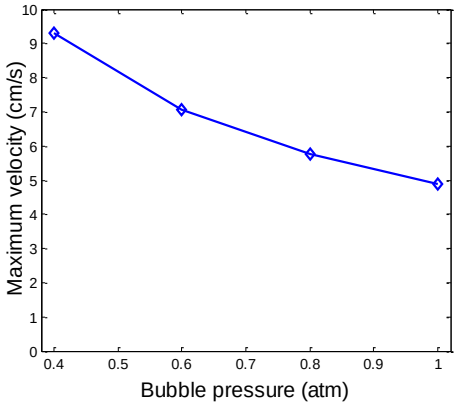

Figure 12. The relationship between the maximum velocity and the bubble pressure.

7. Conclusions

The modeling successfully simulates and predicts the flow behavior of the molten flux and also the magnesium transport during the refining process. It was observed that at the bottom of the of the flux there was a dead zone in which the flux was stagnant. This suggests that design changes to the setup or increasing the rate of stirring may increase the evaporation of magnesium.

In the SOM process, the flux is highly viscous; therefore magnesium transport is significantly higher near the stirring tube during electrolysis. As a result it has been determined that the highest current efficiencies in SOM electrolysis process are obtained when the stirring tube is used as the cathode. The flow behavior of the molten flux at reduced pressure was also simulated. As the pressure of the system drops and the argon bubble size increases the velocity of the flux also increases.

8. References

1. X. Guan, P. A. Zink, U. B. Pal, and A. C. Powell, "Magnesium Recycling of Partially Oxidized, Mixed Magnesium-Aluminum Scrap through Combined Refining and Solid Oxide Membrane Electrolysis Processes," *ECS Transactions*, Vol. 41, No. 31, pp. 91-101, 2012.

2. U. B. Pal and A. C. Powell, "The use of solid-oxide-membrane technology for electro-metallurgy," *Journal of the Minerals, Metals and Materials*, vol. 59, no. 5, pp. 44-49, 2007.

3. A. Krishnan, U. Pal, and X. G. Lu, "Solid oxide membrane process for magnesium production directly from magnesium oxide," *Metallurgical and Materials Transactions B*, vol. 36, no. 4, pp. 463-473, 2005.

4. M. Ek and D. Sichen, "Application of Multiphysics in the Simulation of Metallurgical Processes," *Proceedings of the COMSOL Conference 2010 Paris*, pp. 3-7, 2010.

5. "Flow in a bubble column reactor", *COMSOL Multiphysics Model Gallery*, No. 2160, 2008.

6. A. Krishnan, "Solid Oxide Membrane Process for the Direct Reduction of Magnesium from Magnesium Oxide," Ph.D. Dissertation, Boston University, 2006.

7. E. Gratz, "Solid Oxide Membrane (SOM) Stability in Molten Ionic Flux for the Direct Electrolysis of Magnesium Oxide," Ph.D. Dissertation, Boston University, 2013 (to be published).

9. Acknowledgements

This material is based upon work supported by the Department of Energy under Award No. DE-EE0003454. The authors thank Dr. Adam C. Powell, Steve Tucker, and Dr. Soobhankar Pati. for helpful discussions.